THE YALE JOURNAL OF BIOLOGY AND MEDICINE 61 (1988), 427-446

Glycocalyx Electrostatic Potential Profile Analysis: Ion, pH, Steric, and Charge Effects

JAN E. SCHNITZER, M.D., B.S.E.

Department of Cell Biology, Yale University School of Medicine, New Haven, Connecticut

Received June 8, 1988

The Poisson-Boltzmann equation is modified to consider charge ionogenicity, steric exclusion, and charge distribution in order to describe the perimembranous electrostatic potential profile in a manner consistent with the known morphology and biochemical composition of the cell's glycocalyx. Exact numerical and approximate analytical solutions are given for various charge distributions and for an extended form of the Donnan potential model. The interrelated effects of ionic conditions, bulk pH, ion binding, local dielectric, steric volume exclusion, and charge distribution on the local potential, pH, and charge density within the glycocalyx are examined. Local charge-induced, potential-mediated pH reductions cause glycocalyx charge neutralization. Under certain conditions, local potentials may be insensitive to ionic strength or may decrease in spite of increasing charge density. The volume exclusion of the glycocalyx reduces the local ion concentration, thereby increasing the local potential. With neutral lipid membranes, the Donnan and surface potential agree if the glycocalyx charge distribution is both uniform and several times thicker than the Debye length (~20 Å in thickness under physiological conditions). Model limitations in terms of application to microdomains or protein endo- and ectodomains are discussed.

INTRODUCTION

It has become apparent that characterizing membrane surfaces is instrumental in understanding the underlying principles of a number of biological phenomena. Charged surfaces are ubiquitous in biological systems at all levels of cellular organization. Perimembranous membrane charges affect ion transport [1–4], molecular binding or adsorption [3,5–8], enzyme activity [9–12], transmembrane diffusion potentials [2,3,13], photosynthesis [14,15], fusion [16], electron transfer reactions [15], protein incorporation into membranes [17], adhesion [18], and development [19]. Charge-dependent, potential-mediated pH changes near cell membranes may neutralize local negative charges (possibly altering local molecular conformations) and thereby influence electron transfer reactions [15], ion transport [2], and probably even membrane fusion and protein incorporation into membranes (i.e., translocation). Surface charges contribute both to nonspecific initial membrane surface interactions via long-range forces and to specific interactions on a molecular, short-range basis.

The ectodomains of integral membrane proteins (IMP) and of glycolipids, along with any bound or adsorbed molecules, constitute the cell surface coat called the glycocalyx. Cationized tracers that bind the anionic glycocalyx charges give estimates of the thickness of the glycocalyx charge layer [20,21]. It is now clear that biological

Abbreviations: D.L.T.: double-layer theory IMP: integral membrane proteins PC: phosphatidylcholine PS: phosphatidylserine

Address reprint requests to: Jan E. Schnitzer, M.D., B.S.E., Dept. of Cell Biology, Yale University School of Medicine, P.O. Box 3333, New Haven, CT 06510

membranes and their glycocalyx are non-random, microheterogenous charged structures [22] with a great diversity of ionizable charge sites [23,24]. Transmembrane and lateral heterogeneity of lipid and protein distribution exists in both eukaryotic and prokaryotic membranes [25]. Many cells contain small regions of specialized molecular arrangement called microdomains [22]. To complicate matters further, recent evidence indicates that, within each membrane molecule, charges of both glycolipids [26] and endo- and ectodomains of IMP (for example, low-density lipoprotein receptor [27] and glycophorin [28]) may be distributed non-uniformly. The inherent localized charge distribution within each microdomain/ectodomain determines the local electrostatic potential profile which characterizes the membrane, the surrounding ionic microenvironment, and the general nature of the surface molecular interactions.

Such complexity in membrane surface structure requires an extremely generalized approach to the analysis of the perimembranous electrostatic potential profile. Within its limitations, this analysis examines the ionic microenvironment, potential, and pH within the glycocalyx while maintaining the heterogeneity of both cell surface charge groups and spatial organization. This general approach allows application to a variety of cell surfaces (both intracellular and extracellular), cell organelles, proteoliposomes, microsomes, or protein-coated particles. Numerical and analytical solutions for both a continuum and a Donnan potential model are developed and compared. For the first time, this analysis combines the effects of charge distribution, local potential, pH, local dielectric, local volume exclusion, and ionic microenvironment in a single self-consistent expression. The limitations of the model are discussed in terms of microdomains and IMP ectodomains.

PAST ANALYSIS

Classic Guoy-Chapman double-layer theory (D.L.T.) has been applied successfully to physical electrochemical and colloidal systems, but its strict predictive capability for biological processes has been somewhat limited [18]. The apparent physical incongruity is caused by an uncritical application of an experimentally verified theory of colloidal particle electrokinetics to a dissimilar biological system. In keeping with physical observations of colloidal particles, D.L.T. assumes a homogenous dielectric with charged sites spread uniformly over a single surface plane in a fixed (non-ionogenic) state, which is screened only by electrolyte counter-ions. First, cells differ from colloidal particles by elaborating a cell surface coat of finite thickness composed of glycoproteins and glycolipids that distribute charge through some depth normal to the surface. Only if this charge thickness is significantly less than Debye length can one properly assume a single plane charge distribution. Recently, several studies have considered the distribution of charge normal to the surface [29,30] in relation to cell electrophoresis [31–34]; however, they ignore several other important effects that the glycocalyx may have. Both the space occupied by the molecules of the glycocalyx and electrostatic forces due to glycocalyx charges influence the partitioning of molecules within the glycocalyx [3,6]. For example, the glycocalyx of mucinous cells have large volume exclusions, which decrease the local partitioning of various molecules based on size and charge [35]. In addition, charges of the glycocalyx and lipid surface are not fixed but are dissociable (ionogenic), as indicated by their pH sensitivity. Ions other than protons may also bind these charges [2,5,36–39]. The effects of ionizable groups have been examined only for surface charges in a Guoy-Chapman-Stern type of model [1,2,37]. The glycocalyx also may alter the local mean dielectric within itself. For the

first time, this analysis will combine all of these factors (charge distribution normal to the surface, charge ionogenicity, dielectric variation, and volume exclusion) into a single, self-consistent expression.

MATHEMATICAL ANALYSIS

This mathematical analysis applies the fundamental principles of classic D.L.T. in a general manner consistent with the known structural morphology and biochemical composition of the cell's glycocalyx. The basic assumptions of D.L.T. are discussed well elsewhere [3,37]. The Poisson-Boltzmann equation is modified to include the ionogenic charge distribution function of the glycocalyx, the volume exclusion of the glycocalyx as it affects the exclusion of ions within the glycocalyx, and any change in mean dielectric within the glycocalyx. The charged region adjacent to the lipid bilayer, whether extracellular or intracellular, contains multiple ionogenic charged sites determined by the particular population of IMP, glycolipids, or any bound molecules. This charged region may be uniformly distributed over an effective charge thickness (d) or may involve more complicated charge distributions such as charged layers or bands. The surface charges of the phospholipid membrane are treated as ionogenic sites evenly distributed over a flat, planar structure. As an alternative to this continuum model, a Donnan potential model is created, utilizing the same modified Poisson-Boltzmann equation with different boundary conditions.

Potential Profile Analysis

A general form of the Poisson equation describes the relation between local charge distribution (ρ) and the mean local electrostatic potential (Ψ) as:

$$\nabla \cdot (-\epsilon \nabla \Psi) = \Sigma \rho_i(x) = \rho_t(x) \tag{1}$$

where ϵ is the local mean dielectric constant, and ρ for any charged species (i) is expressed as a function of distance x, starting at the lipid membrane surface. The parameters, x, ϵ, Ψ, and ρ, are rendered dimensionless by division with κ^{-1}, ϵ_b, kT/e, and eI, respectively. The Debye length (κ^{-1}) is defined as $(4\Pi e^2 I/\epsilon_b kT)^{-1/2}$, where e is the electron charge, k is the Boltzmann constant, T is the absolute temperature, ϵ_b is the bulk dielectric, and I is $N\Sigma z_i^2 c_i$ with N, z, and c being Avogadro's number, charge valence, and concentration, respectively. The total charge density distribution ($\rho_t(x)$) is the sum of every charged species in the ionic diffuse double layer ($\rho_d(x)$) and in the glycocalyx around the cell ($\rho_g(x)$). The diffuse double layer contains the screening ions surrounding the charged sites. These ions distribute within any volume (i.e., glycocalyx), depending on both the steric and electrostatic partition functions. The ion concentration within the glycocalyx is hindered sterically by any molecules occupying space within the glycocalyx (i.e., ectodomains of IMP). The steric partition function (Φ_s) for a permeant molecule within a random meshwork of membrane molecules is [40]:

$$\Phi_s = \exp(-v_e^o) \exp[(v_e^o - v_e^r)/(1 - v_e^o)] \tag{2}$$

where v_e is the normalized volume exclusion for either a point molecule (superscript o) or a molecule of radius r (superscript r). The v_e^r is dependent on the specific geometry of the membrane and the partitioning molecule [40]. For a spherical ion of radius (r_p) interacting with glycocalyx molecules modeled as cylindrical fibers of mean radius (r_f), $v_e^r = v_e^o(1 + r_p/r_f)^2$ [40]. If ions are treated as point charges and if volume exclusion is

small, Φ_s becomes equal to 1 minus the volume occupied by the molecules of the glycocalyx relative to the total volume of the glycocalyx ($1 - \nu_e^o$). Ions partition electrostatically (Φ_e) according to a Boltzmann distribution based on the local potential [37]. Since the total partition function [$\Phi = c_g/c_b$, where c is the concentration of any molecule in the glycocalyx (subscript g) or in the bulk solution (subscript b)] equals $\Phi_s\Phi_e$, equation 1 becomes:

$$\nabla \cdot (-\epsilon \nabla \Psi) = \rho_t(x) = \rho_g(x) + NI^{-1} \sum_{i=1}^{n} z_i c_i \Phi_{s_i} \exp(-z_i \Psi) \tag{3}$$

Glycocalyx Charge Density Analysis

The glycocalyx consists of both cationic and anionic dissociable, pH-sensitive charge groups. The total charge will be the summation of the different ionizable groups such as specific acidic and basic amino acids:

$$\rho_g(x) = I^{-1} \left\{ \sum_{j=1}^{m} \alpha_{bj}[B_j^*(x)] - \sum_{i=1}^{n} \alpha_{ai}[A_i^*(x)] \right\} \tag{4}$$

where [ ] denotes the volumetric concentration of either basic (B) or acidic (A) groups in the glycocalyx as a function of position, the superscript * denotes the maximum number of available ionogenic sites, α is the fraction dissociated as indicated by: $\alpha_{ai} = [A_i(x)]/[A_i^*(x)] = K_{ai}/(K_{ai} + [H])$ and $\alpha_{bj} = [B_j(x)]/[B_j^*(x)] = [H]/(K_{bj} + [H])$, and K is the equilibrium dissociation constant for either acids (a) or bases (b). For a uniform or band-like charge distribution, the volumetric charge concentration is the total number of charges of a given species per unit surface area (σ_g), divided by the thickness of distribution of that charge within the glycocalyx (d_i). Since the local hydrogen ion concentration ($[H]$) is dependent on the local potential (see equation 10), the local glycocalyx charge density ($\rho(x,\Psi)$) is a function of both x and Ψ:

$$\rho_g(x,\Psi) = I^{-1} \left\{ \sum_{j=1}^{m} \frac{[H]_b[B_j^*(x)]}{K_{bj}e^{\Psi} + [H]_b} - \sum_{i=1}^{n} \frac{K_{ai}[A_i^*(x)]}{K_{ai} + [H]_b e^{-\Psi}} \right\} \tag{5}$$

Extension of this analysis to include the binding of other ions is simple; however, the paucity of data precludes a meaningful analysis.

Membrane Surface Charge Analysis

Consistent with past approaches, the membrane lipid surface is treated as a uniformly smeared charge plane[1] [2,3,6]. Unlike the condition for the glycocalyx, equilibrium binding constants [5,38,39] are available on the binding of various ions to anionic phospholipids such as phosphatidylserine (PS) and to neutral lipids such as phosphatidylcholine (PC). A trivial extension of the analysis used to derive equation 5 yields both a general expression for proton binding to acidic and basic moieties and a

[1]An alternate approach to the charges of the lipid membrane simply involves distributing the charge within the polar region of the bilayer so that σ_s located at the surface of the hydrocarbon region is zero [4]. Thus, the charge may be treated as part of the glycocalyx charge density function ($\rho(x)$).

specific expression for *Na*, *H*, and *Ca* binding to PS and PC membranes:

$$\sigma_s = d_s^{-2} = (\kappa/I)\left\{\sum_{j-1}^{m} \frac{[H]_b[B_{sj}^*(x)]}{K_{sbj}e^{\Psi} + [H]_b} - \sum_{i-1}^{n} \frac{K_{sai}[A_{si}(x)]}{K_{sai} + [H]_b e^{-\Psi}}\right\}$$

$$\sigma_s = (\kappa/I) \cdot \left\{\frac{-[\mathrm{PS}]}{1 + [H]_b e^{-\Psi_s}/K_H^{ps} + [Na]e^{-\Psi_s}/K_{Na}^{ps} + [Ca]e^{-2\Psi_s}/K_{Ca}^{ps}} + \frac{2[\mathrm{PC}]}{1 + K_{Ca}^{pc}e^{2\Psi_s}/[Ca]}\right\} \tag{6}$$

where σ_s is the surface charge normalized by multiplication with κ/Ie. A 1:1 stoichiometry for Na-PS and Ca-PC binding is assumed, while Ca-PS association is 2:1. The σ_s is the inverse of the mean surface charge separation distance (d_s) squared.

Surface Potential and Electric Field Analysis

Gauss's theorem of electrostatics gives the boundary condition at the surface ($x = 0$) and at the outer glycocalyx perimeter ($x = d$) as:

$$\epsilon_{s-}\nabla\Psi|_{s-} - \epsilon_{s+}\nabla\Psi|_{s+} = \sigma \tag{7}$$

where $s+$ and $s-$ indicate which side of the surface plane that $\nabla\Psi$ and ϵ are evaluated, and σ is the planar charge evaluated at $x = 0$ ($\sigma = \sigma_s$) or at $x = d$ ($\sigma = 0$). Equations 3 and 5 integrated once using the usual boundary conditions (as x approaches ∞, Ψ and $\nabla\Psi$ equal 0) combined with equation 7 evaluated at $x = d$ so that:

$$(\nabla\Psi)^2 = 2NI^{-1}\sum_{i-1}^{p} c_i\Phi_{s_i}[e^{-z_i\Psi} - 1 + (1 - \epsilon_g^2)e^{-z_i\Psi_d}]$$
$$+ 2I^{-1}\left\{\sum_{j-1}^{m}[B_j^*(x)]\ln\left[\frac{K_{bj} + [H]_b e^{-\Psi}}{K_{bj} + [H]_b e^{-\Psi_d}}\right] + \sum_{i-1}^{m}[A_i^*(x)]\ln\left[\frac{[H]_b + K_{ai}e^{\Psi}}{[H]_b + K_{ai}e^{\Psi_d}}\right]\right\} \tag{8}$$

where Ψ_d is the potential at $x = d$ and ϵ_g is the mean dimensionless dielectric in the glycocalyx.

Combination of equations 6, 7, and 8 results in a complete, exact nonlinear solution for the surface potential (Ψ_s) that considers the effects of charge distribution, volume exclusion, dielectric variation, and charge ionogenicity. Given Ψ_d, an iterative solution is possible via trial and error or via more elegant numerical techniques [41].

Possible Solutions

Exact analytical solutions of equation 3 or equation 8 are not tractable. The analytical solutions for approximations of equation 3 are developed fully in Appendix A. They consider the volume exclusion, dielectric, and bulk pH effects but ignore the potential-mediated dissociative effects on the charge density. Solutions for different charge distributions are given in the appendix, including planar, band-like (multilayers), and uniform.

There are several possible approaches [41,42] in deriving a unique numerical solution of the potential profile given by equation 3 or equation 8. In order to provide the least ambiguity and best precision in this analysis, a boundary value problem [41,42] is developed using equation 3 combined with equation 5 by utilizing the electric field boundary conditions at $x = 0$ (equations 6 to 8) and $x = d$ (equation 8). This

solution works well under most conditions; however, as d becomes small and/or the potential large, the nonlinearity of these equations causes difficulties. Therefore, another numerical paradigm was created. It requires boundary potentials, Ψ_s and Ψ_d. Ψ_s is calculated iteratively via combination of equations 6 to 8 with Ψ_d approximated by equation A4, A5, A6, or A7 depending on the charge distribution. Ψ_d is reguessed until the electric fields given by equation 8 agree with the values given by the numerical solution (relative error 10^{-4}). Hence, the final unique solution satisfies the potential continuity condition at $x = d$ along with the Gaussian electric field condition (equation 7) both at $x = 0$ and $x = d$. Outside the glycocalyx, the numerical solution is continued with the requirement that Ψ and $\nabla\Psi = 0$ as x approaches ∞.

Donnan Potential Analysis

The classical derivations of the Donnan potential (Ψ_D) assume an equilibrium between two infinitely large reservoirs separated by a membrane which is impermeable to only a single charged solute located in one of the reservoirs. The continuum at the interfacial region is ignored. The bulk ion concentration in each reservoir is calculated from the difference between the mean bulk potentials in the two reservoirs away from the interface [37]. Electroneutrality is required in each reservoir and the ion concentrations are defined by Boltzmann distributions. The electroneutrality requirement may be expressed as $\int \rho_i(x)dx = 0$ in each reservoir so that, via equation 3, a constant potential profile within each reservoir is predicted since $\epsilon\nabla\Psi = 0$. Within the framework of these assumptions, a constant potential and dielectric within each reservoir makes $\nabla(\epsilon\nabla\Psi) = 0$ so that the modified Poisson-Boltzmann equation, as defined by equation 3 with equation 5, describes the Donnan potential as:

$$NI^{-1}\sum_{i-1}^{n} z_i c_i \Phi_{s_i} \exp(-z_i\Psi_D) = \sum_{i-1}^{w} \frac{K_{ai}[A_i^*]}{K_{ai} + [H]_b e^{-\Psi_D}} - \sum_{j-1}^{m} \frac{[H]_b[B_j^*]}{[H]_b + K_{bj}e^{-\Psi_D}} \quad (9)$$

which may be solved iteratively for Ψ_D. If we ignore the ioniogenic effects so that $\rho(\Psi) = \rho_{gk}$, for a univalent electrolyte $\Psi_D = \sinh^{-1}(\rho_{gk}/\Phi_s)$, which reduces to an expression developed by others [30,37] when $\Phi_s = 1$. For low potentials ($|\Psi_D| < 1$) $\Psi_D \approx \rho_{gk}/\Phi_s$. Thus, Ψ_D becomes dependent on the impermeant charge density within the reservoir and the relative volume available to the ions within the reservoir. The well-known quadratic equation for the Donnan equilibrium for ions can be easily derived as $c_D = c_i[\rho_{gk} + (\rho_{gk}^2 + 1)^{1/2}]$ assuming a Boltzmann distribution for the ions and $\Phi_s = 1$. This equation is only an approximation, based on a fixed charge model accurate only at low ρ_{gk}, at Φ_s near 1, and when pK $\ll$ pH. Outside the glycocalyx, a true Donnan model requires that the potential be constant (reference $\Psi = 0$) so that a discontinuity in potential exists at the interface ($x = d$). For comparison purposes, however, the potential outside the glycocalyx is solved as per the continuum model either numerically or via equation A2 where Ψ_D replaces Ψ_s.

RESULTS AND DISCUSSION

Microdomain/Glycocalyx Potential Profiles

Figure 1 compares two exact nonlinear numerical solutions for the potential profile with the linearized approximate solution (equation A5) under different surface charge conditions. One exact solution assumes fixed, non-ionogenic anionic sites ($\rho_g(x,\Psi) = \rho_{gk}$ = constant in equation 3), while the other includes ionogenic effects (equation 5).

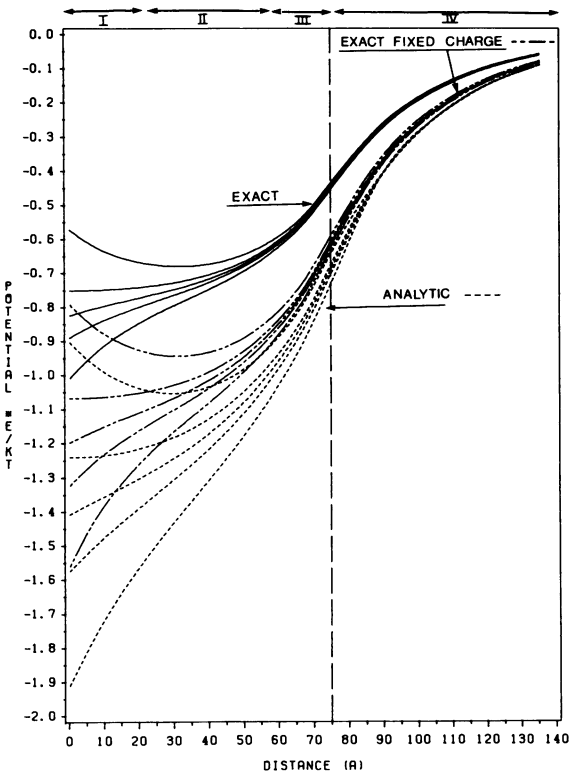

FIG. 1. Comparison of three possible solutions of glycocalyx potential profile. The glycocalyx thickness is 75 Å with 4×10^7 anions per cell. Cell surface area is 163 μm^2. Thus, the glycocalyx charge density is 6.54×10^{19} charges/cm^3 (110 mEq/l). The bulk pH equals the charge pK (3.4). The [NaCl] is .01 M. The potential is expressed in dimensionless units where one unit is about 25 mV at room temperature. The three sets of curves represent the ionogenic (equations 3 and 5) and fixed charge (equation 3, $\rho_g = \rho_{gk}$) exact solution and the linearized approximate solution (equation A5). For each group of curves, the lipid membrane surface charge is altered and is a fraction of the total glycocalyx charge. In descending order, the surface charge is +.10, 0, −.05, −.10, and −.20 of the total glycocalyx charge. The glycocalyx volume exclusion (v_e^o) is 0.05 and is assumed to be a meshwork of cylindrical fibers with a radius of 5 Å. The radius of Na and Cl are assumed equal at 2 Å. The dashed vertical line at $x = 75$ Å indicates the outer border of the glycocalyx.

The chosen physical parameters of the glycocalyx are consistent with the known values for the erythrocyte [28,31,43]. For each case, both fixed charge solutions significantly overestimate the local potential, especially as the lipid surface charge increases. These discrepancies are greatest near the lipid surface ($x = 0$). Under these conditions, errors exceeding 40 percent and 70 percent are noted for the fixed charge exact and linear solutions, respectively. The exact, pH-sensitive solution results in smaller increases in Ψ_s because, as Ψ increases with greater ρ (lower ionic strength or increased charge density), the charge-dependent, potential-mediated pH reduction at the surface significantly neutralizes the nearby charges. Under conditions where $\Psi \leq 1$ (low ρ_g or large I) and pK $\ll$ pH$_b$ so that local pH effects are negligible, all three solutions agree.

For the linear and fixed charge solution, Fig. 1 shows that the potential at the outer periphery of the glycocalyx is approximately half the surface potential when no lipid charge exists. As a result of the exponential terms in equation A5, whenever the glycocalyx charge thickness is greater than the Debye length ($d \gg 1$), the analytical solution reduces to $\Psi_s = \rho_{gk}$ and $\Psi_d = \rho_{gk}/2$. As shown by the exact solution in Fig. 1, however, Ψ_d may become significantly greater than half of Ψ_s because of greater charge neutralization near the membrane surface from the lower local pH (pH$_s$ < pH$_d$).

For a homogeneous glycocalyx charge distribution of constant charge density, the potential profile is strongly influenced by d. This phenomenon is expressed analytically in equation A5. As d decreases, the glycocalyx charge effect on Ψ_s decreases,

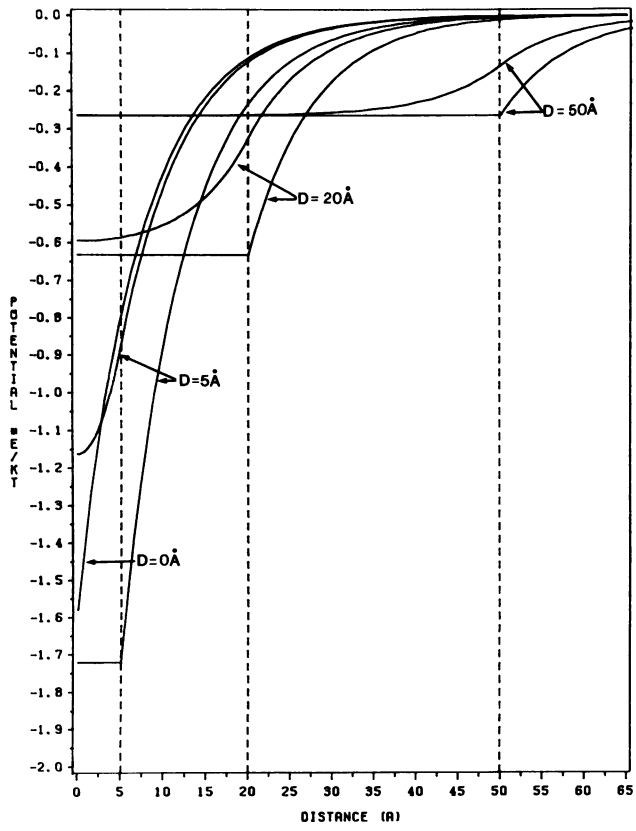

FIG. 2. The effect of the glycocalyx charge thickness (D) on the perimembranous potential profile. Also, a comparison of the continuum versus the Donnan model. The total number of anionic sites per surface area (same as Fig. 1) is constant. The charges are distributed uniformly but within variable thicknesses. The bulk pH is 7.4 and the pK of the charges is 3.6. The [NaCl] = .15 M. The three dashed vertical lines represent the outer glycocalyx edge for their respective curves. Each D has two curves, except for $D = 0$. The curves with the constant, flat glycocalyx potential profile are from the Donnan model (equation 9). The other curves are based on the ionogenic continuum model expressed in the numerical solution of equation 3 with equation 5.

eventually approaching zero as d approaches zero (no charge); however, as shown in Fig. 2 (continuum model), if the number of anionic charge sites per surface area of cell membrane (σ_g) is constant, then as d decreases, the charge density ($\rho_g = \sigma_g/d$) and the surface potential increase until ultimately, for $d = 0$, all of the charge is at the lipid surface ($\sigma_s = \sigma_g$). In fact, for small d ($d = 5$Å in Fig. 2) the potential profile almost overlaps with the planar surface charge model ($d = 0$) except within the first 2–3 Å of the surface, where the local difference is about 25 percent. For lower ionic strengths, however, for bulk pH values closer to the pK, or for situations where other ions bind either the surface or glycocalyx charges, the sensitivity of the surface potential to d decreases. As expected, the diminution of d increases the local glycocalyx potentials; however, this increase results in greater local proton/ion concentrations that bind and neutralize the membrane charges. As will become more apparent in the forthcoming discussion, this ion binding may result in a saturation type of phenomenon that tends to keep local potentials constant.

As shown in Figs. 1 and 2 and typified by equation A5, the potential profile of a uniformly charged glycocalyx (with $d \gg 1$) can be analyzed in terms of three or four regions. Starting at the lipid surface, the potential may decay rapidly (region I) as modeled by the σ_s term in equation A5. Clearly, the lipid surface charge density significantly influences the potential profile. A positive surface charge, which may occur under special conditions of Ca-lipid interactions, may cause the potential profile to become concave upward, with a maximum negative potential inside the glycocalyx.

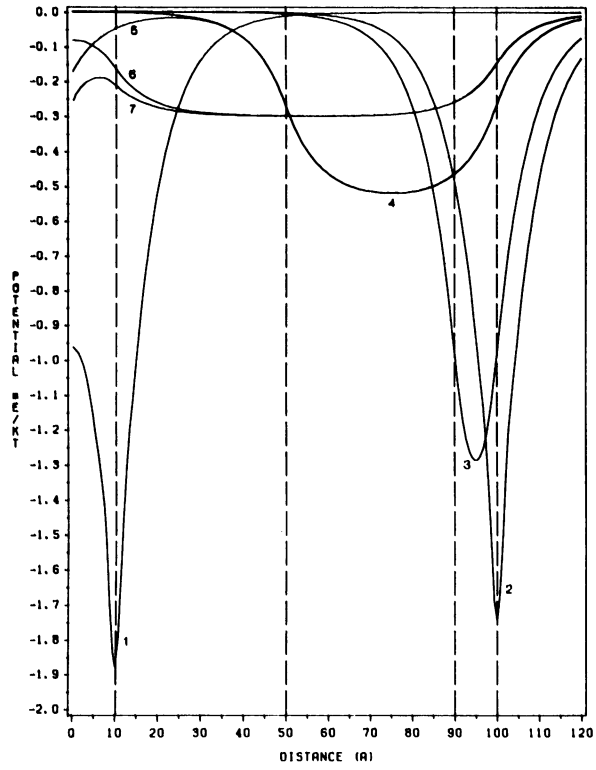

FIG. 3. Effects of non-uniform glycocalyx charge distribution on the potential 7 profile. The total glycocalyx thickness is 100 Å with 8×10^7 anionic sites per cell. Surface area is 163 μm^2. The bulk pH is 7.4. The pK of the charge sites is 3.4. The [NaCl] is .15 M. The dashed vertical lines represent boundaries for the various charge bands. Curves 1 and 2 have all the charge distributed in a plane with one located 10 Å from the surface and the other at 100 Å from the lipid surface. Curve 3 results from charge distributed over the last 10 Å of the glycocalyx. Curves 4 and 5 have the charge in the outer half (50 Å) of the glycocalyx with curve 5 also having an additional 10 percent of the glycocalyx charge at the lipid surface. Curves 6 and 7 have all the charge distributed over the outer 90 Å of the glycocalyx with curve 7 having the same surface charge as in curve 5. The vertical dashed lines indicate the band edges for the various charge distributions.

The slope at $x = 0$ indicates the sign and magnitude of a plateau region (II) evident where the electric field approaches zero. If the lipid surface is neutral, the plateau phase starts at the surface. At the outer periphery of the glycocalyx, a large potential drop occurs (region III). Outside the glycocalyx in the bulk extracellular environment (region IV), the potential decays almost exponentially and approximates zero usually within three or four Debye lengths. The relative dimension of each region within the glycocalyx depends on the effective glycocalyx charge thickness, bulk pH and pK of the charges, surface charge, glycocalyx volume exclusion, local dielectric, and ionic strength of the solution. The length of region II increases with d, by either increasing glycocalyx charge thickness, increasing ionic strength, or adjusting any parameter that decreases the Debye length. Smaller Debye lengths decrease the length of the other regions. The potential profile exhibits more complex behavior at pH values near the pK values of the glycocalyx charge sites (Fig. 1 versus Fig. 2). The plateau region becomes less distinct, especially with significant lipid membrane surface charge.

If σ_g is constant, the distribution of the charges within the glycocalyx determines the potential profile. Figure 3 illustrates the effects of different band distributions of glycocalyx charge on the potential profile under equal charge conditions. As the charge is spread uniformly over a smaller part of the glycocalyx, the maximum potential increases and the length of the plateau region decreases. The maximum potential reaches a peak when all the charge is located in one plane. As the planar charge approaches the lipid surface, its peak potential increases (curve 2 versus curve 3), reaching its greatest value when it is at the lipid surface (data not shown).

The effect of glycocalyx charges on the surface potential is a function of the charge

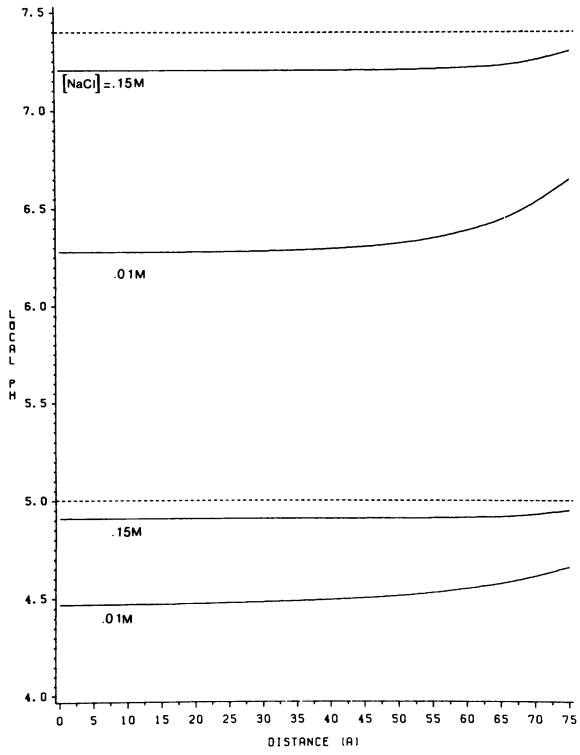

density and distribution and of the ionic conditions as they affect the Debye length. Significant glycocalyx charge may not affect surface potentials. For diffuse, moderately charged band profiles, the glycocalyx charge affects surface potential when it is distributed homogeneously throughout the glycocalyx (Figs. 1 and 2) or when the band edge is within one or two Debye lengths of the membrane surface (Fig. 3, curves 1, 6, 7). Comparison of the various potential profile curves shows that the greatest effect on the surface potential occurs when the glycocalyx charge is condensed within a single thin band and is located within a few Debye lengths of the surface (10–20 Å for physiologic ionic conditions). This distance increases with salt reduction.

Experimental data support these theoretical predictions. Anionic glycolipids significantly alter lipophilic ion adsorption [44,45]. This effect was greater for anionic phospholipids, an observation consistent with the anionic site(s) in gangliosides being located several Å from the lipid membrane surface. X-ray diffraction [26] and electrokinetic [36] studies of gangliosides embedded in bilayer membrane show that the sialic acid is located 10 Å from the lipid surface in a planar distribution.

Glycocalyx/Microdomain pH and Charge Density Profile

The local potential and pH are important factors determining the behavior of the membrane. Past analysis of membrane surface pH assumed either a Donnan type of potential or a surface potential from an impenetrable planar surface charge [3,15,37]. With a charged layer such as a glycocalyx, however, it is necessary to know the local pH distribution. An accurate assessment must include proton binding to charge sites.

The significance of dissociable charged groups on cell surfaces becomes more

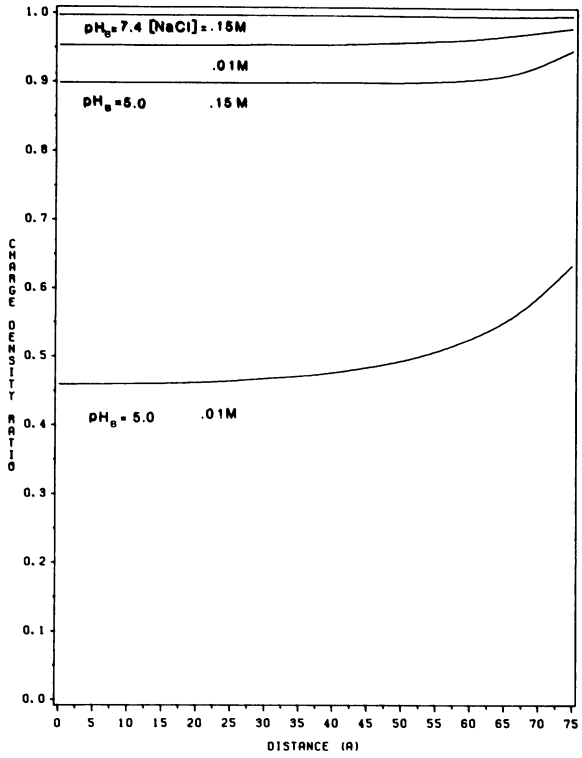

FIG. 4. Effects of pH_b and [NaCl] on the pH and charge profile within the glycocalyx. The glycocalyx/microdomain charge characteristics are the same as in Fig. 1 except that the charge pK is 5. The lipid surface charge is zero. **A.** The pH profile is at two different bulk pH conditions (7.4 and 5.0, indicated by the dashed straight lines) for different [NaCl]. **B.** Charge profile. The charge density ratio is the calculated local charge density (equation 5), divided by the charge density corrected for pH_b effects alone (equation 5 with $\Psi = 0$).

apparent with increasing surface potentials. A negative surface potential results in the accumulation of cations at the surface. Since the proton concentration is usually several orders of magnitude less than other cation concentrations in solution, it classically is ignored. In a pH-sensitive biomolecular system, however, local changes in pH may neutralize local charge. The local pH (pH_x) is derived from the Boltzmann equation for hydrogen ions: $[H]_x = [H]_b \exp(-\Psi)$ which in terms of pH becomes:

$$pH_x = pH_x + \Psi/\ln 10 \tag{10}$$

For a local potential of about -60 mV ($\Psi = 2.3$), a drop of one pH unit can be expected. With an anionic glycocalyx, the negative potential results in a drop in the local perimembranous pH and in greater protonation of the anionic charges. Since the isoelectric point (pI) of many cells and even of cell organelles is within two pH units of 7.4 [25], local charge-induced, potential-mediated pH effects should be considered in evaluating perimembranous electrostatic effects.

Figure 4A shows the pH profile inside the glycocalyx, while Fig. 4B illustrates the charge density profile for uniformly distribued anionic charges. The local pH is lowest at the lipid surface ($x = 0$). The surface pH can be reduced further by an anionic phospholipid membrane. Both the pH and charge density are relatively constant until they increase gradually in the outermost quarter of the glycocalyx. The charge effects on both the local pH and potential-mediated charge neutralization (see also Fig. 6 where Ψ_s mimics pH_s as shown by equation 10) is greatest under conditions which increase the local ρ and Ψ such as greater charge density or lower ionic strength. Charge neutralization is most significant when the local pH is near the pK of any of the

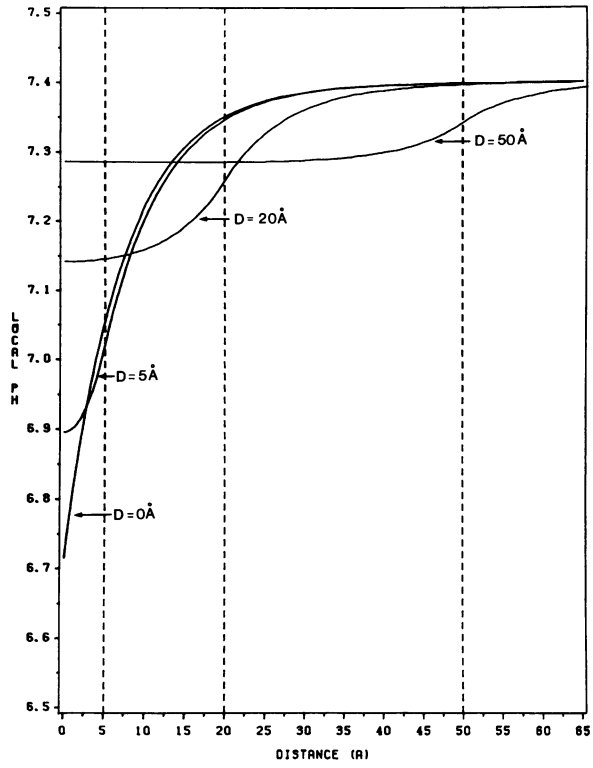

FIG. 5. Effect of glyocalyx charge thickness (D) on the pH profile. Conditions are as in Fig. 2.

charged moieties of the glycocalyx. On the other hand, as the pH approaches the pK, the local bulk pH difference decreases, due to the smaller overall charge density and local potential.

The charge density distribution significantly affects the pH profile. Figure 5 shows the effect that the glycocalyx charge thickness has on the pH profile. As d decreases, the local potentials within the glycocalyx increase (see Fig. 2) resulting in greater pH reduction. The surface pH is lowest if $d = 0$ where all the charge is distributed in a plane on the surface. The perimembranous pH profile duplicates the shapes of the potential profile curves because of the linear nature of equation 10. This fact is evident in comparing Figs. 2 and 5. The more complicated potential profiles of Figs. 1 and 2 also demonstrate the pH profile with Ψ_s at $x = 0$ yielding pH_s (via equation 10) and as x becomes large, $\Psi = 0$ so that $pH_x = pH_b$.

Ion Effects on Surface Potential and Glyxoxalyx Charge Density

The solid curves of Fig. 6 illustrate the effects of both pH and salt concentration on the potential at the cell/microdomain/ectodomain surface. Several of the iso-osmolar curves show that Ψ_s saturates when the pH is two units greater than the charge pK, similar to classic equilibrium titration curves. At low salt concentrations, however, a quasi-linear relation is found in the pH range shown. Saturation is not reached three pH units above the charge pK. Since the Debye length in solutions without salt at pH 8.0 is about 3 μm and is about 8 Å for .15 M NaCl, it is not surprising that rather large potentials (> -250 mV) are reached with little or no salt in solution. With a large diminution in salt concentration, the proton becomes not only the charge-neturalizing,

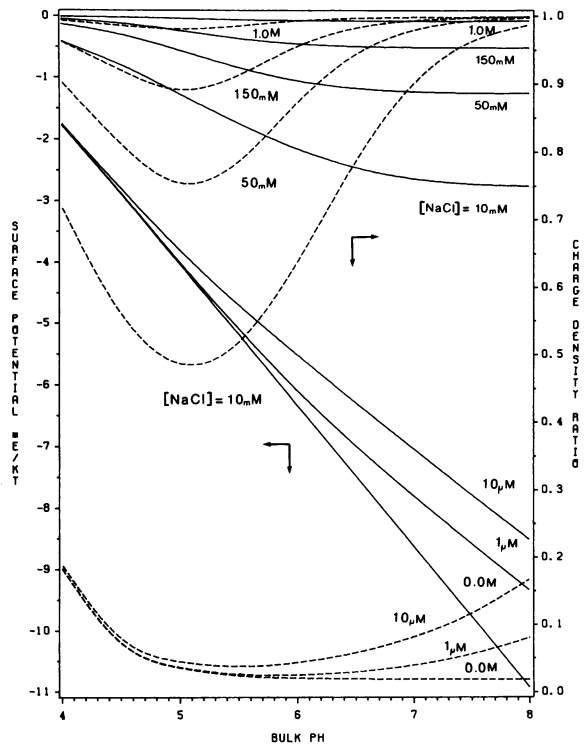

FIG. 6. Effects of pH and electrolyte concentration on the surface potential and glycocalyx charge density using the exact ionogenic numerical solution. The cell surface microdomain has a uniform charge density of 9.82×10^{18} charges/cm^3 (16 mEq/l) with pK of 5.0. The effective glycocalyx charge thickness is 50 Å. The curves are at different electrolyte concentrations, as indicated.

binding ion but also the most significant screening counter-ion. As discussed previously, if ionogenic effects are ignored, several-fold greater potentials are predicted (data not shown).

The pH change within the glycocalyx must alter the charge density of ionogenic sites, especially when the ambient pH is near the pK of the charged group. The dashed lines of Fig. 6 show the effect of glycocalyx charge density of potential-mediated pH changes at the membrane surface as a function of bulk pH and salt concentration. For a given pH, the charge density is expressed as a fraction between 0 and 1. At high salt concentration (1 M), the charge density ratio is about 1, so that the bulk solution pH predominantly determines the glycocalyx charge density. As the electrolyte concentration diminishes, however, significant potential-mediated charge neutralization occurs for any given pH_b. For each isomolar curve the pH at which a minimum density ratio ($\approx$pK) is reached increases as the salt concentration decreases. No distinct minimum is reached within the pH range tested for zero salt concentration.

Interestingly, the surface potentials shown in Fig. 6 at negligible salt concentrations indicate that the surface pH calculated via equation 10 is almost constant ($pH_s \approx 3$) with bulk pH variation. The large surface potentials cause charge neutralization even when the pH is far greater than the pK of the charged species. The surface pH is quite constant from pH 5 to 8, indicating a fixed surface pH and charge density at negligible electrolyte concentrations. Under these conditions, the local surface pH is buffered to pH = 3 by the surface charges.

Because Ψ and ρ are interrelated, the dashed curves in Fig. 6 give an accurate depiction of when it is important to consider potential-mediated pH effects: in other words, conditions under which the exact ionogenic and exact fixed charge solutions are

equivalent. Clearly, the discrepancy increases with ionic strength diminution. At 10 mM NaCl, the effect becomes small when the pH is two to three units above the pK. Even though the charge density used in this example is quite small at about 15 percent of that of an erythrocyte, it is a significant function of ionic strength, of charge distribution and density, and of the pH_b-pK difference. Many cells have far greater charge densities [24]. Greater charge only amplifies these effects, with charge neutralization becoming significant at higher ionic strengths and at greater pH_b-pK differences.

Comparison to the Donnan Potential Model

The glycocalyx charges, if uniformly distributed, may be interpreted as equivalent to the solute impermeant charges of the Donnan model, resulting in a constant potential within the glycocalyx, as shown in Fig. 2. Such an analysis creates a discontinuity of the electric field at the glycocalyx outer border (a physical inconsistency unless a plane charge is present). Under certain conditions, however, the Donnan potential overlaps the continuum model potential, especially near the cell membrane surface. After comparing the nonlinear, ionogenic potential profiles of the continuum model with the Donnan model shown in Fig. 2 and comparing the linearized analytical expressions for Ψ (equation A5) and Ψ_D, it is clear that $\Psi_s \approx \Psi_D$ if the glycocalyx charge is distributed uniformly over a large thickness ($d \gg 1$) around a neutral membrane surface ($\sigma_s = 0$). A comparative analytical expression is derived by dividing equation A5 by the Ψ_D analytical expression (assuming Ψ_D decreases exponentially outside the glycocalyx): for $x \leq d$, $\Psi(x)/\Psi_D = 1 - \exp(-d)\cosh(x)$ and for $x \geq d$, $\Psi(x)/\Psi_D = (1 - \exp(-2d))/2 \approx 0.5$. As illustrated by these equations and by Fig. 2, if $d \gg 1$, $\Psi(x)$ and Ψ_D agree over most of the glycocalyx; however, as x increases, the difference increases, with Ψ_D becoming about twice the value of $\Psi(x)$ at $x = d$. Under these specific conditions, these analytical equations and the numerical solutions of the ionogenic, nonlinear equations establish the equivalence of Ψ_s and Ψ_D for $d \geq 3$ (10 percent error) which, under physiological conditions, is about 20 Å. If the charge density is sufficient to create large potentials, one must consider the ionogenic effects included in equation 9 to calculate Ψ_D, especially if the pK of the charge site is near the pH_b.

If an appreciable lipid surface charge exists or if the glycocalyx charge distribution is not uniform, $\Psi_s \neq \Psi_d$. With discontinuous glycocalyx charge distribution, such as a band of charge, Ψ_D may be calculated given ρ_g within the band. This Ψ_D becomes equivalent to the plateau potential within the bands (see Fig. 3, curves 4, 5, 6, 7) only if the normalized band thickness is three to four times greater than the Debye length ($d > 3$). As shown in curve 3, a plateau potential is not seen as the band thickness decreases. Even when Ψ_D does equal the plateau potential, it cannot be considered uniform throughout the band (curve 4). *In any continuous or discontinuous uniform charge distribution, Ψ_D appropriately mimics local potentials only if the local electric field approaches zero and remains zero within the surrounding two or three Debye lengths.*

Regulation of Cell Membrane Microenvironment

The details provided by this analysis on effects of charge on local potentials, pH, and ion concentrations furnish a physicochemical basis for understanding how cells may regulate their own microenvironments by controlling both the charge and volume

exclusion (i.e., via glycosylation) of their surface proteins. Indeed, under low salt conditions *Escherichia coli* secretes up to 16 times more of a highly anionic membrane-derived oligosaccharide into the periplasmic space than under normal conditions [46]. This secretion provides a homeostatic mechanism for maintaining the necessary ionic conditions (i.e., osmolarity) in the periplasm for cell survival. Could similar charge density changes occur in other cells or even within particular ectodomains of cell IMP under variable ionic conditions, especially to cells normally subjected to large ionic changes?

Model Limitations

The spatial heterogeneity of charge distribution varies between microdomains and even between surface molecules. This proposed analysis for potential profile can be used for individual microdomains or for single IMP endo- or ectodomains if the lateral dimension in the plane parallel to the plasmalemma is significantly greater than the Debye length. The Debye length is about 8 Å under physiologic conditions and increases to about 100 Å in .001 M salt. Microdomains [22] and many IMP ectodomain dimensions [26,27,28] meet this requirement. Although this analysis should be precise in the central core region, the influence of the environment laterally surrounding the microdomain increases as one moves away from the central core region toward the periphery. Within two or three Debye lengths of the microdomain or ectodomain border, significant contribution from the lateral surroundings must exist [47].

The assumption of smeared charge distribution within the glycocalyx or even within bands may be suspect under certain conditions [48]. More sophisticated multidimensional analyses are possible, such as the approximate solution to the Poisson equation developed for examining the electrostatic potential profile of proteins [49] and the exact numerical solution to the Poisson-Boltzmann equation applied to ion channel analysis [47]. Detailed data on discrete charge localization and local dielectrics are not available, however, for membrane proteins. Intuitively, discrete charge effects should be most prominent under conditions of high ionic strength and low charge [48].

This type of theoretical analysis has many applications which may increase our understanding of electrostatic effects on cell surface phenomena.[2] Now that the assumptive handcuffs of past analyses using D.L.T. have been released, more precise, consistent, and logical applications to biological systems on a cellular level are possible.

APPENDIX A

Various analytical expressions that approximate the exact numerical solution developed in the main body of the text are derived, based on various simplifying assumptions.

Glycocalyx Free Regions

For the case of charge located only at the lipid surface, the complexity of the solution is reduced greatly. In equation 8, the glycocalyx charge density term is zero and both Φ_s

[2]Recently, this approach has been extended to analyze possible steric and electrostatic effects on the cooperative binding of molecules within the glycocalyx [6] and has been broadened to both two- and three-dimensional analysis to examine ion interactions with lipid membranes and ion channels [47].

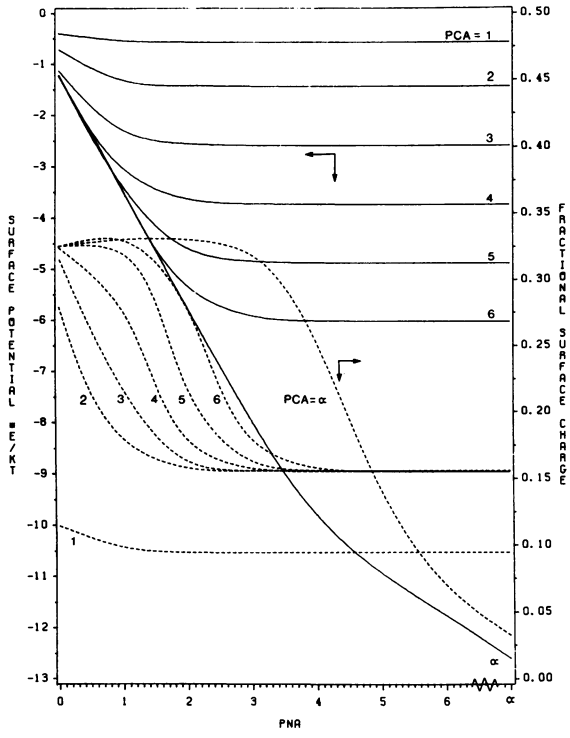

FIG. A1. Surface potential and charge dependence on electrolyte concentration for 100 percent PS membranes without a glycocalyx. There is one PS molecule per 70 Å^2. The pH is 7.2. pNa and pCa are the negative logarithms of Na and Ca concentrations, respectively. The solid curves represent the surface potential, while the dashed curves represent the fraction of the total available surface charge dissociated, both as a function of pNa at a given pCa. The dissociation constants for Na and Ca binding to PS are 1.67 M and 0.33 M, respectively [5]. The intrinsic proton pK for the carboxyl group of PS is 3.6 [39].

and $\epsilon_g = 1$ so that, combined with equation 7, one gets:

$$\sigma_s^2 = 2NI^{-1} \sum_{i=1}^{n} c_i[\exp(-z_i\Psi) - 1] \qquad \text{(A1)}$$

Ψ_s is calculated iteratively, using equations 6 and A1. This solution is equivalent to the Guoy-Chapman-Stern solution [1,37]. With Ψ_s calculated and for a simple 1:1 electrolyte, the potential is expressed by the well-known analytic solution [37]:

$$\Psi(x) = 2 \ln [(1 + e^{-x} \tanh(\Psi_s/4))/(1 - e^{-x} \tanh(\Psi_s/4))] \qquad \text{[A2]}$$

For more complex ionic conditions, a boundary value numerical solution is used with $\Psi = \Psi_s$ at $x = 0$ and $\Psi = 0$ as $x \Longrightarrow \infty$.

Figures A1 and A2 show the effects of monovalent and divalent ion binding on both the surface charge and potential. Both monovalent and divalent ions bind to lipid membranes, resulting in significant charge neutralization. The dashed curves show the effect of [NaCl] on the fractional surface charge of PS membranes at different [CaCl]. The solid curves of Figs. A1 and A2 show the dominating effect that Ca ions have on Ψ_s at various [NaCl]. Without Ca ions present, Ψ_s increases rapidly with diminution of [NaCl]. Under certain conditions with Ca present, large plateau regions of constant Ψ_s are seen irrespective of [NaCl]. This effect is directly attributable to the divalent nature of the ion, resulting in greater screening efficiency, surface concentration, and binding affinity for PS. Since low [CaCl] may maintain a constant local Ψ, it is important to reduce [CaCl] to zero or at least to know it accurately; otherwise one may incorrectly conclude that charge effects are insignificant. In comparison with

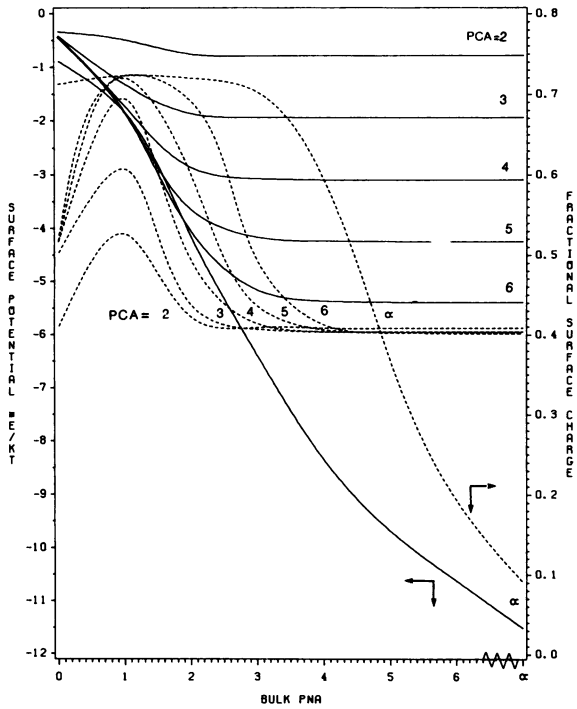

FIG. A2. Surface potential and charge dependence on electrolyte concentration for 20 percent PS membranes. There is one PS molecule per 350 Å^2. Other conditions are as in Fig. A1.

D.L.T., potential-dependent charge neutralization from ion binding tends to maintain lower and sometimes constant local Ψ (data not shown).

Linearized Fixed Charge Profile

Equation 3 is linearized by Taylor series expansion of the exponential term. The glycocalyx charge density (ρ_{gk}) is assumed to be independent of Ψ by setting $\Psi = 0$ in equation 5 so that it depends only on x and pH_b. The mean dielectric is assumed to be constant throughout the glycocalyx. For a 1:1 electrolyte solution with Φ_s being equal for both ions, one gets this linear second-order differential equation:

$$\nabla^2\Psi = (\Phi_s\Psi - \rho_{gk})/\epsilon_g \qquad [A3]$$

which is solved satisfying the usual boundary conditions at $x = 0$ and $x = \infty$:

$$\Psi(x) = (\sigma_s e^{-mx})/m + (m/\Phi_s)\cosh(mx)\int_0^d e^{-mx}\rho_g(x,\mathrm{pH}_b)\,dx - (e^{mx}/2)\int_0^x e^{-mx}\rho_g(x,\mathrm{pH}_b)\,dx + (e^{-mx}/2)\int_0^x e^{mx}\rho_g(x,\mathrm{pH}_b)\,dx \qquad [A4]$$

where $m = (\Phi_s/\epsilon_g)^{1/2}$. All of the integral forms are dependent on the glycocalyx charge distribution profile. If the charges are uniformly smeared throughout the glycocalyx, one gets, using the appropriate boundary conditions at $x = d$ (continuity of Ψ and equation 7):

$$\Psi(x) = \sigma_s e^{-mx}/m + \rho_{gk}\Gamma[1 - \Gamma\cosh(mx)]/\Phi_s \qquad 0 \le x \le d$$
$$\Psi(x) = \sigma_s e^{-mx}/m + \rho_{gk}\Gamma\sinh(md)e^{d-x}/(m\Phi_s) \qquad 0 \le x \le d \qquad [A5]$$

where $\Gamma = [\cosh(md) + \sinh(md)/m]^{-1}$. For a given bulk pH, ρ_g is a constant (ρ_{gk}), which is the total number of glycocalyx charges per unit surface area (σ_g), divided by the effective glycocalyx charge thickness ($\rho_{gk} = \sigma_g/d$). Equation A5 reduces to past analytical solutions if the dielectric, steric exclusion, and bulk pH effects are ignored [31,32,34].

For the case of non-uniform charge distribution in the glycocalyx, analytical solutions are still tractable under the same assumptions, but the boundary conditions must be different. If the charge (σ_b) is located in a plane at $x = b$ away from a charged lipid surface, the usual boundary conditions at $x = 0$ and ∞, coupled with equation 7 at $x = b$, may be used so that if both ϵ and $\Phi_s = 1$ then:

$$\begin{aligned} \Psi(x) &= \sigma_s e^{-x} + \sigma_b e^{-b} \cosh(x) && 0 \le x \le b \\ \Psi(x) &= [\sigma_s + \sigma_b \sinh(b)]\, e^{-x} && x \ge b \end{aligned} \qquad \text{[A6]}$$

If the charge is spread in the glycocalyx in a band-like distribution only between planes located at $x = a$ and $x = b$ away from the membrane, the general solution requires three equations:

$$\begin{aligned} \Psi(x) &= \sigma_s e^{-x} + \rho_{gk}[e^{-a} - e^{-b}] \cosh(x) && 0 \le x \le a \\ \Psi(x) &= \sigma_s e^{-x} + \rho_{gk}[1 - e^{-b} \cosh(x) - e^{-x} \sinh(a)] && a \le x \le b \\ \Psi(x) &= [\sigma_s + \rho_{gk}(\sinh(b) - \sinh(a)]e^{-x} && x \ge b \end{aligned} \qquad \text{[A7]}$$

where $\rho_{gk} = \sigma_g/(b - a)$. As a approaches b so that a plane charge exists, the solution reduces to equation A6, as expected. If $a = 0$, one gets a simplified form of equation A5. Furthermore, in the extreme where the glycocalyx charge approaches the cell surface and becomes planar, the solution reduces to the well-known, linearized, flat-plate exponential solution [37].

For a charge distribution with several bands of different charge density located in the glycocalyx, this approach is generalized to yield:

$$\begin{aligned} \Psi(x) &= C_1 e^{-x} + D_1 e^{x} + \rho_{gk1} && 0 \le x \le x_1 \\ \Psi(x) &= C_n e^{-x} + D_n e^{x} + \rho_{gkn} && x_{n-1} \le x \le x_n \\ \Psi(x) &= F e^{-x} && x \ge x_n \end{aligned} \qquad \text{[A8]}$$

with

$$C_1 = D_1 + \sigma_s \quad \text{and} \quad C_n = (D_n - D_{n-1}) \exp(2x_{n-1}) + C_{n-1}$$

$$D_n = \rho_{gkn} \exp(-x_n)/2 \quad \text{and} \quad D_{n-1} = D_n + (\rho_{gkn} - \rho_{gkn-1}) \exp(-x_{n-1})/2$$

$$F = C_n - D_n \exp(2x_n)$$

where the numbered subscript signifies each charge band starting at the lipid membrane surface. From these equations, a simplified form of equation A5 is found if $n = 1$. Equation A7 is found for $n = 2$ with $x = a$ and $x = b$ and with $\rho_{gk1} = 0$.

For each of the above analytical expressions, σ_s may be replaced by equation 6 and the resultant equation solved iteratively for Ψ_s with $x = 0$. For $x > 0$, σ_s remains constant as determined by Ψ_s and the equation is solved as usual. This expression at least partially considers ionogenic effects at the surface. σ_b can also be expressed similarly to equation 6 and solved iteratively in equation A6 using Ψ at $x = b$.

ACKNOWLEDGEMENTS

This work is supported in part by NIH grant HL-17080 and by a gift from RJR Nabisco, Inc.

This work was presented in part at the Biophysical Society Meeting, San Francisco, California, February 1986, and at the Microcirculatory Society Meeting, St. Louis, Missouri, April 1986.

REFERENCES

1. Gilbert DL, Ehrenstein G: Use of a fixed charge model to determine the pK of negative sites on the external membrane surface. J Gen Phys 55:822–825, 1970
2. Bell JE, Miller C: Effects of phospholipid surface change on ion conduction in the K^+ channel of sarcoplasmic reticulum. Biophys J 45:279–287, 1984
3. McLaughlin S: Electrostatic potentials at membrane-solution interfaces. Curr Top Membr Transp 9:71–144, 1977
4. Schnitzer J: A mathematical analysis of lipid charge effects on electrophoresis, hydrophobic ion adsorption, and membrane conductance. Biophys J 49:515a, 1986
5. Ohki S, Kurland R: Surface potential of phosphatidylserine monolayers. II. Divalent and monovalent ion binding. Biochim Biophys Acta 645:170–176, 1981
6. Schnitzer J, Carley W: Electrostatic and steric partition function of the endothelial glycocalyx. Fed Proc 45:1152, 1986
7. Schnitzer J, Carley W: Rat serum albumin binding of rat epididymal fat pad endothelial cells in culture. Fed Proc 46:1541, 1987
8. Schnitzer J, Carley W, Palade GE: Specific albumin binding to microvascular endothelium in culture. Am J Physiol 254:H425–H437, 1988
9. Ahrens M: Electrostatic control by lipids upon the membrane bound (Na^+-K^+)-ATPase II. The influence of surface potential upon the activating ion equilibria. Biochim Biophys Acta 732:1–10, 1983
10. Cunningham CC, Sinthusek G: Ionic charge on phospholipids and their interaction with the mitochondrial adenosine triphosphatase. Biochim Biophys Acta 350:150–153, 1979
11. Nalecz MJ, Zborowski J, Famulski KS, Wojtczak L: Effect of phospholipid composition on the surface potential of liposomes and the activity of enzymes incorporated into liposomes. Eur J Biochem 112:75–80, 1980
12. Wojtczak L, Nalecz MJ: Surface charge of biological membranes as a possible regulator of membrane-bound enzymes. Eur J Biochem 94:98–107, 1979
13. Gilbrat R, Grignon C: Effect of pH on the surface charge density of plant membranes: comparison of microsomes and liposomes. Biochim Biophys Acta 692:462–468, 1982
14. Barber J: Membrane surface charges and potentials in relation to photosynthesis. Biochim Biophys Acta 594:253–308, 1980
15. Conjeaud H, Mathis P: Electron transfer in photosynthetic membrane: Influence of pH and surface potential on the P-680 reduction kinetics. Biophys J 49:1215–1221, 1986
16. Poste G, Allison AC: Membrane fusion. Biochim Biophys Acta 300:421–465, 1973
17. Eytan GD, Bronza R: Role of charge and fluidity in the incorporation of cytochrome oxidase into liposomes. J Biol Chem 9:3196–3203, 1978
18. Weiss L: Biophysical aspects of initial cell interactions with solid surfaces. Fed Proc 30:1649–1657, 1971
19. Jaffe LF: Electrical controls of development. Ann Rev Biophys Bioeng 6:445–476, 1977
20. Billings-Galgiardi S, Pockwinse SW, Schneider GB: Surface coats on human lymphocytes: Freeze drying and staining with cations. Am J Anat 154:267–276, 1981
21. Nicholson GL: Anionic sites of human erythrocyte membranes. I. Effects of trypsin, phospholipase C, and pH on the topography of bound positively charged colloidal particles. J Cell Biol 57:373–387, 1973
22. Palade GE: Differentiated microdomains in cellular membranes: current status. In The Cell in Contact. Edited by GM Edelman, JP Thiery. New York, John Wiley and Sons, 1985, pp 9–24
23. Stoltz JF, Nicolas A: Analytical study of ionized or ionizable groups of platelet membrane. Blut 38:103–117, 1979
24. Sherbert GV: The Biophysical Characterization of the Cell Surface. New York, Academic Press, 1978
25. Karnovsky MJ, Kleinfeld AM, Hoover RL, Dawidowicz EA, McIntyre DE, Salzman EA, Klausner RD: Lipid domains in membranes. Ann NY Acad Sci 401:60–75, 1982
26. McDaniel RV, McIntosh TJ: X-ray diffraction studies of the cholera toxin receptor G. Biophys J 49:94–96, 1986

27. Goldstein JL, Brown MS, Anderson RGW, Russell DW, Schneider WJ: Receptor-mediated endocytosis: Concepts emerging from LDL receptor systems. Ann Rev Cell Biol 1:1–39, 1985
28. Viitala J, Jarnefelt J: The red cell surface revisited. Trends Biochem Sci 10:392–395, 1985
29. Parsegian VA: Possible modulation of reactions on the cell surface by changes in electrostatic potential that accompany cell contact. Ann NY Acad Sci 238:362–371, 1972
30. Ohshima H, Ohki S: Donnan potential and surface potential of a charged membrane. Biophys J 47:673–678, 1985
31. Donath E, Pastushenko V: Electrophoretical study of cell surface properties. The influence of the surface coat on the electric potential distribution and on general electrokinetic properties of animal cells. Bioelectrochem and Bioenerg 6:543–554, 1979
32. Jones IS: A theory of electrophoresis of large colloidal particles with adsorbed polyelectrolyte. J Coll Interf Sci 68(3):451–461, 1979
33. Sharp KA, Brooks DE: Calculation of the electrophoretic mobility of a particle bearing bound polyelectrolyte using the nonlinear Poisson-Boltzmann equation. Biophys J 47:563–566, 1985
34. Wunderlich RW: The effects of surface structure on the electrophoretic mobilities of large particles. J Coll Interf Sci 88:385–397, 1982
35. Polefka TG, Garrick RA, Redwood WR, Swislocki NI, Chinard FP: Solute-excluded volumes near the Novikoff cell surface. Am J Physiol 247:C350–C356, 1984
36. McDaniel R, McLaughlin S: The interaction of calcium with gangliosides in bilayer membranes. Biochim Biophys Acta 819:153–160, 1985
37. Davies JT, Rideal EK: Interfacial Phenomena. New York and London, Academic Press, 1961
38. McLaughlin A, Grathwohl C, McLaughlin S: The adsorption of divalent cations to phosphatidylcholine bilayer members. Biochim Biophys Acta 513:338–357, 1978
39. Tsui FC, Ojcius DM, Hubbell WL: The intrinsic pK values for a phosphatidylserine and phosphatidylethanolamine in phosphatidylcholine host bilayers. Biophys J 49:459–468, 1986
40. Schnitzer JE: Analysis of steric partition behavior of molecules in membranes using statistical physics: application to gel chromatography and electrophoresis. Biophys J, in press
41. Gerald CF, Wheatley PO: Applied Numerical Analysis. Reading, MA, Addison-Wesley Publishing Inc, 1984
42. Lapidus L, Pinder GF: Numerical Solution of Partial Differential Equations in Science and Engineering. New York, John Wiley and Sons, Inc, 1982
43. Eylar EH, Madoff MA, Brody OV, Oncley JL: The contribution of sialic acid to the surface charge of the erythrocyte. J Biol Chem 237(6):1992–2000, 1962
44. Usai C, Robello M, Gambale F, Marchetti C: Effect of gangliosides on phospholipid bilayer: A study with the lipophilic ion relaxation method. J Memb Biol 82:15–23, 1984
45. Feinstein MB, Spero L, Felsenfield H: Interaction of a fluorescent probe with erythrocyte membrane and lipids: Effects of local anesthetics and calcium. FEBS Lett 6:245–248, 1970
46. Kennedy EP: Osmotic regulation and the biosynthesis of membrane-derived oligosaccharides in Escherichia coli. Proc Natl Acad Sci USA 79:1092–1095, 1982
47. Schnitzer JE, Lambrakis CC: Multi-dimensional numerical solutions for electrostatic interaction of charged molecules with lipid membranes and ion channels. Biophys J 53:399a, 1988
48. Brown RH: Membrane surface charge: Discrete and uniform modelling. Progr Biophys Mol Biol 28:343–370, 1974
49. Warwicker J, Watson HC: Calculation of the electric potential in the active site cleft due to alpha helix dipoles. J Mol Biol 157:671–679, 1982